Gas Sensors Based on Metal Oxide Nanowire Bundles: Preparation and I-V Characterization

A. Ponzoni, A. Vomiero, E. Comini,
M. Ferroni, G. Faglia, G. Sberveglieri

CNR-INFM SENSOR, Chemistry and Physics Department of Brescia University
Via Valotti 9, 25133 Brescia, Italy

Metal oxides have been recently synthesized as quasi one-dimensional single crystalline nanostructures, such as nanowires, nanobelts, nanotubes, nanorods [1].

Several works have demonstrated a strict relation between the structural features of such materials and their innovative properties, suited for the development of different devices such as nano-transistors, field-emitters, nanocantilevers, gas-sensors [2].

Despite the exciting results obtained in several fields, including nano-electronics, the preparation of electrical contacts to integrate nanowires in functional devices remains a challenging task. Furthermore, it is fundamental to identify how the electrodes affect the device properties. It has been shown in literature that the resistance of a device based on a single semiconducting nanowire is strongly dominated by the reverse-biased junction formed at the nanowire-electrode interface [3].

In this work we focus on metal oxide nanowire bundles which have been largely investigated as gas sensors, but few works have been addressed to identify the contribution of the electrical contacts [4] (and references therein).

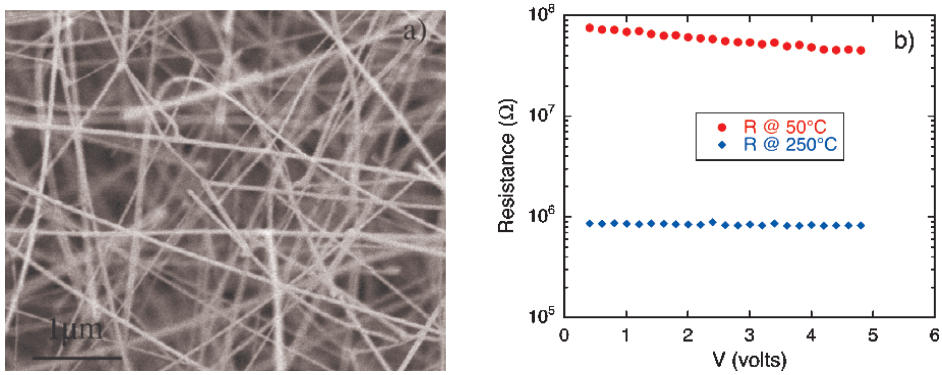

Figure 1: (a) Secondary-electron SEM image of a nanowire bundle; (b) device resistance (R) plotted as a function of the applied voltage; the voltage dependence of R indicates that the contribution of the electrode-nanowire junction affects the device resistance at low temperature (50°C) while it becomes negligible at high temperature (250°C and above)

We use a lift-off method based on a sacrificial SiO_2 layer to pattern the nanowire growth according to the device layout. Electrodes are further deposited by sputtering.

The effectiveness of the method to prepare reliable contacts is verified by means of I-V characterization. An analysis of the temperature dependent I-V relationship permits to identify the conditions (bias voltage and sensor temperature) in which the device conductance can be ascribed to the nanowire bundle rather than to the electrode-nanowire junction.

Acknowledgements
This work was partly supported by the NATO project no. 982166 "Chemical threat detectors based on multisensor arrays and selective porous concentrators" and, within the EU FP6, by the ERANET project "NanoSci-ERA: NanoScience in the European Research Area".

References

[1] Pan Z W, Dai Z R, Wang Z L 2001 *Science* **291** 1947
[2] Wang Z L, Liu Y, Zhang Z (Eds) 2003 *Handbook of nanophase and nanostructured materials*, Tsinghua University Press, Vol. 3 and 4
[3] Hernandez-Ramirez F et al 2007 *Phys. Rev. B* **76** 085429
[4] Comini E et al 2009 *Progr. Mater. Sci.* **54** 1

Hydrogenation of Thin Mg Films in $CH_4 + Ar$ Plasmas

L. Pranevicius[1], D. Milcius[2], C. Templier[3], L. L. Pranevicius[1,2], A. Bacianskas[1]

[1] *Department of Physics, Vytautas Magnus University 8 Vileikos St., LT-44404 Kaunas, Lithuania*

[2] *Centre for Hydrogen Energy Technologies, Lithuanian Energy Institute 3 Breslaujos St., LT-44403 Kaunas, Lithuania*

[3] *Université de Poitiers SP2MI, Bd Marie et Pierre Curie, 30179 Futuroscope, France*

Storage of hydrogen at near ambient temperatures and pressures is an unsolved problem for the scientific community. Hydride storage in solids is one of the most promising, safe solutions for sustainable use. The magnesium and its alloys have attracted a lot of attention since the gravimetric hydrogen capacity is relatively high 7.6 wt. % for Mg, 3.6 wt. % for Mg_2Ni and the systems are reversible. However, hydrogen loading kinetics is slow. The accommodation efficiency of equilibrium molecular hydrogen in metals and alloys is extremely low in comparison with that of the non-equilibrium hydrogen. In the present work, plasma technologies are used when activated hydrogen particles with the efficiency close to 1 are accommodated in the metal lattice, or just stick to its surface, depending neither on the temperature nor on the atomic composition of metal samples.

The non-equilibrium plasma immersion ion implantation technique was used in an attempt to produce new alloys and compounds with new structures modifying and altering their thermodynamic properties. Hydrogenation of 1.5–2 μm thick Mg films deposited on quartz and stainless steel substrates was performed in the range of low (370–420 K) temperatures using $CH_4 + Ar$ working gas in the range of 0.1–5 Pa pressures. Mg films were immersed in plasma and ions were extracted from the plasma by applying a high (0.5–2 kV) pulsed voltage. After hydrogenation, the depth across film thickness distributions of H and C atoms was measured using the Elastic Recoil Detection Analysis (ERDA) with 35 MeV Cl^+. The phases were identified using X-ray diffraction (XRD) technique and the surface topography of as-deposited and hydrogenated films was analyzed by scanning electron microscopy.

The experimental carbon distribution profiles were fitted with the simulated ones based on the analysis of solutions of rate equations describing a variety of processes, such as carbon adsorption, diffusion, sputtering, ion implantation and ion mixing. The dominant mechanisms transporting incident particles from the surface into the bulk are discussed.

The study aims at finding plasma treatment parameters for the realization of magnesium hydrogenation using CH_x compounds as the working gas, so as to avoid the hydrogen purification process.

A X-ray Absorption Spectroscopy Study of a Low-Pt Content Nano-catalyst Operating in a PEM Fuel Cell

E. Principi[1], A. Witkowska[2], S. Dsoke[3], R. Marassi[3], A. Di Cicco[1,4]

[1] *CNISM, Department of Physics, University of Camerino*
Via Madonna delle Carceri 9, I-62032 Camerino (MC), Italy

[2] *Department of Solid State Physics, Gdansk University of Technology*
Narutowicza 11/12, 80-233 Gdansk, Poland

[3] *Department of Chemistry, University of Camerino*
Via S. Agostino 1, I-62032 Camerino (MC), Italy

[4] *IMPMC-CNRS UMR 7590, Université P. et M. Curie*
140 rue de Lourmel, 75015 Paris, France

An X-ray absorption spectroscopy (XAS) study of a novel Pt-based catalyst layer (Pt loading 0.1 mg/cm^2) operating at the cathode of a proton exchange membrane fuel cell (PEMFC) is presented. This innovative catalyst is based on the use of a mesoporous inorganic matrix as a support for the catalyst nanoparticles. The catalytic efficiency thus obtained has been found to be comparable to state-of-the-art electrodes with a Pt loading of 1 mg/cm^2.

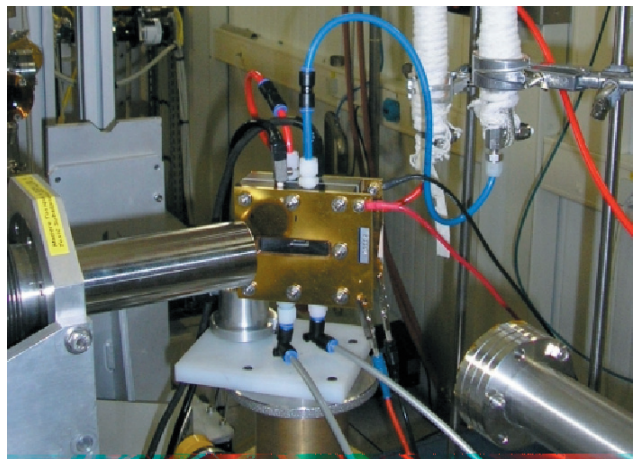

Figure 1: Picture taken at the BM29 spectrometer (ESRF) showing the special PEM fuel cell positioned close to the 13-channels Ge X-ray detector (on the left) on the beam direction

Due to the very low Pt content, in-situ measurements of its structural properties by XAS are challenging and suitable experimental strategies must be devised for this purpose. In particular, it is shown that accurate XAS in-situ fluorescence measurements can be obtained using an optimized fuel cell, suitable protocols for alignment of a focused x-ray beam and an appropriate filter for the background signal of other atomic species contained in the electrode. Details, advantages and limitations of the XAS technique for the in-situ measurements are discussed. An analysis of the near-edge XAS and EXAFS (extended X-ray absorption fine structure) data shows that Pt nanoparticles have a local structure compatible with that of bulk Pt (fcc) and the coordination numbers match those expected for particles with typical sizes in the 1.5 nm range. Changes in the oxidation state and in the local disorder are found for different applied potentials. The catalyst support, containing W atoms, exhibits a partial reduction upon the PEMFC activation thus mimicking the catalyst behavior. This indicates a possible role of the mesoporous matrix in favoring the oxygen reduction reaction (ORR) and stimulates further research on active catalyst supports [1].

References

[1] Principi E., Witkowska A., Dsoke S., Marassi R. and Di Cicco A., submitted to Phys. Chem. Chem. Phys. 2009

Nanostructured Titania Photoanodes for Dye-sensitized Solar Cells: Optimization of Deposition Techniques

L. Vesce[1,2], R. Riccitelli[1,2], A. Reale[1,2], T. M. Brown[1,2], A. Di Carlo[1,2]

[1] *CHOSE – Centre for Hybrid and Organic Solar Energy Via G. Peroni 400, 00197 Rome, Italy*

[2] *Electronic Eng. Dept., University of Rome Tor Vergata Via del Politecnico, 1, 00133 Rome, Italy*

The development of the dye-sensitized solar cell (DSC) requires optimization of several materials that are involved in the photoelectrochemical process of the cell. Among the different steps in the realization of efficient DSCs, it is the control of the quality, morphology and design of the nanoporous titania layer that is of fundamental importance. A highly porous nanocrystalline TiO_2 film (with a large effective surface area) is typically optimized in recent designs by a light-scattering layer. The TiO_2 film is prepared using the techniques of screen-printing for nanocrystalline and submicron-crystalline TiO_2 film layers as well as a chemical bath deposition for $TiCl_4$ treatment [1].

The photon-trapping effect can be induced by the use of a combination of a transparent nanocrystalline TiO_2 film with a microcrystalline light-scattering layer [2,3], in conjunction with an anti-reflecting film (ARF) [4] and other techniques [5], thus enhancing IPCE. The $TiCl_4$ treatment is usually adopted as pre- and post-treatment for the TiO_2 deposition, since the pre-treatment influences positively the bonding strength between the fluorinated tin oxide (FTO) substrate and the porous TiO_2 layer, and blocks the charge recombination between electrons emanating from the FTO and the $I^{3\pm}$ ions present in the $I^{\pm}/I^{3\pm}$ redox couple. The post-treatment enhances the surface roughness factor and the necking of the TiO_2 particles, thus augmenting the dye adsorption; this results in higher photocurrent.

Spectroscopic techniques can be used to monitor IPCE, and 2D photocurrent maps can be helpful to control the working electrode uniformity that depends strongly on the deposition techniques.

Acknowledgements
We acknowledge the support Regione Lazio.

References

[1] S. Ito, P. Liska, R. Charvet, P. Comte, P. Péchy, Md. K. Nazeeruddin, S. M. Zakeeruddin, M. Graetzel, Chem. Commun. (2005) 4351
[2] P. Wang, S. M. Zakeeruddin, P. Comte, R. Charvet, R. Humphry-Baker, M. Graetzel, J. Phys. Chem., B 107 (2003) 14336

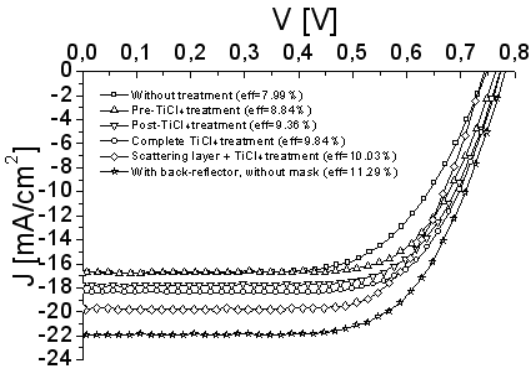

Figure 1: Effects of TiO_2 optimization. Details of cell preparation: the substrates are 8 Ω/sq FTO-glass (2×2 cm^2, Pilkington) cleaned in an ultrasonic bath for 10 min in acetone and for 5 min in ethanol. 0.5×0.5 cm TiO_2 films (thickness $\approx$ 15 μm) deposited via blade coating using Dyesol DSL 18 NR-T TiO2 paste, dried for 5 minutes at 65°C and then sintered at 525°C for 30 min. After sintering the transparent substrates were soaked in a 0.5 mM N719 (Solaronix) dye solution in ethanol for 15 h, and then rinsed in ethanol. The counterelectrodes were prepared by brushing a Pt precursor solution (Platisol, Solaronix) onto the FTO-coated substrates and then annealed at 400°C for 5 minutes. The cells were completed by sealing together the two electrodes via a 60 μm thick Surlyn gasket. Dyesol HPE electrolyte was inserted into the cell via vacuum backfilling. The "pre-treated" cells had the first $TiCl_4$ treatment after the cleaning step. The "post-treated" cells had $TiCl_4$ treatment after transparent TiO_2 sintering step. The pre- and post-treatment is complete treatment. The scattering layer is deposited after $TiCl_4$ "post-treatment". The cells are measured without masking.

[3] DOI: 10.1109/WCPEC.2006.279340
[4] S. Ito, T. Murakami, P. Comte, P. Liska, C. Graetzel, M. Nazeeruddin, M. Graetzel, Thin Solid Films 516/14 (2008) 4613
[5] H Aggelund App. Phys. Lett 92 (2008) 013113, DOI: 10.1063/1.2830817

Percolation in Polymer–Solvent Systems. A Computer Simulation Study

P. Adamczyk[1], P. Polanowski[2], A. Sikorski[1]

[1] *Department of Chemistry, University of Warsaw*
Pasteura 1, 02-093 Warsaw, Poland

[2] *Department of Molecular Physics, Technical University of Łódź*
Żeromskiego 116, 90-924 Łódź, Poland

The percolation in systems containing long flexible polymer chains with explicit solvent molecules was investigated in this work. The polymer chains were represented by linear sequences of lattice points restricted to a two-dimensional triangular lattice. The Monte Carlo simulations were performed applying the cooperative motion algorithm. The percolation thresholds and the critical exponents of chains and solvent molecules were determined and the influence of the chain length on the percolation was discussed. It was shown that the percolation threshold deceased strongly with the chain length what was closely connected with changes in the chain structure with the decreasing polymer concentration. The critical exponents for all chains under consideration and for solvent molecules were found almost constant and close to the theoretical values.

Hybrid Functional Study of Prototypical Multiferroic Systems

A. Stroppa, S. Picozzi

CASTI Regional Laboratory, Consiglio Nazionale delle Ricerche
Instituto Instituto Nazionale di Fisica della Materia (CNR-INFM)
67100 L'Aquila, Italy

We present a detailed study of the structural, electronic, magnetic and ferroelectric properties of prototypical multiferroic systems such as BiFeO3 and orthorombic $HoMnO_3$ [1] using the Heyd-Scuseria-Ernzerhof hybrid functional (HSE) [2]. It has been shown that the HSE functional enables accurate computations on complex systems, such as defects, [3,4] and compounds containing strongly localized electrons, such as *d*- and *f*-electrons, [5] where traditional DFT may be inadequate. Furthermore, it gives a very accurate description of optical properties of many insulating compounds [5].

In this study, by comparing our results with the available experimental data, as well as with the state-of-the-art GW calculations, we show that the HSE formalism is able to account well for the relevant properties of these multiferroic compounds. Furthermore, the correction for the self-interaction error introduced by the exact exchange makes the formalism very appealing for studying more complex materials involving *f*-electrons. Preliminary results are also discussed for $DyFeO_3$. Our conclusions corroborate and complement the emerging evidence of the possibility of predictive first-principles investigations on multiferroic systems using the HSE hybrid functional.

References

[1] Yamauchi K., Sanyal B., Sergienko I. A., Dagotto E., Picozzi S., 2007 *Phys. Rev. Lett.* **99** 227201
[2] Heyd J., Scuseria G.E., and Ernzerhof M. 2003 *J. Chem. Phys.* **118** 8207; Heyd J. and Scuseria G.E. 2004, *ibid.* **120** 7274; Heyd J. and Scuseria G.E. 2004, *ibid.* **121** 1187
[3] Stroppa A. and Kresse G. 2008 *Phys. Rev. B (R)* **79** 201201
[4] Paier J., Stroppa A., Kresse G. and Marsman M. 2008 *J. Phys.: Condens. Matter.* **20** 064201
[5] Janesko B. J., Henderson T.M., Scuseria G. 2009 *Phys. Chem. Chem. Phys.* **11** 443

Effect of Magnetic Anisotropy on the Inverse Superconducting Spin-switch in LCMO-YBCO-LCMO Hybrids

C. Visani[1], N. Nemes[1], M. Rocci[1], Z. Sefrioui[1], C. Leon[1], J. Santamaria[1], M. G. Hernandez[2], S. G. E. te Velthuis[3], A. Hoffmann[3], J. W. Freeland[3], M. R. Fitzsimmons[4], F. Simon[5], T. Feher[5]

[1] *GFMC, Departamento de Fsica Aplicada III, Universidad Complutense de Madrid Madrid, Spain*

[2] *Instituto de Ciencia de Materiales de Madrid, CSIC, Cantoblanco, Spain*

[3] *Materials Science Division, Argonne National Laboratory Argonne, Illinois, USA*

[4] *Los Alamos National Laboratory, Los Alamos, New Mexico, USA*

[5] *Budapest University of Technology and Economics and Condensed Matter Physics Research Group, Hungarian Academy of Sciences, Budapest, Hungary*

The realization of high quality interfaces in superlattices combining manganites and high TC superconductors has open the way to the study of the interplay between half metallic ferromagnetism and non conventional superconductivity. The giant magnetoresistance found in these samples along the superconducting transition may be of interest in the search for new concepts of spintronic devices. In this presentation we will describe the magnetic and transport response of, $La_{0.7}Ca_{0.3}MnO_3$ / $YBa_2Cu_3O_7$ / $La_{0.7}Ca_{0.3}MnO_3$ heterostructures. Combined ferromagnetic resonance, SQUID magnetometry, polarized neutron reflectivity, and magnetic circular dichroism have been used to characterize the magnetic structure. The hybrids show a resistance switching between high and low resistance states, controlled by the biaxial anisotropy of the LCMO electrodes which may be useful for complex oxide-based magnetic memory elements. The high-resistance state appearing when the magnetic layers are antiparallel aligned can be stabilized in a wide field range by applying magnetic field along the [110] easy axes direction. We will show that this property of the F/S/F hybrids displays memory effects which can be used to design a superconducting memory concept. Both the writing and the reading operation can be achieved with a high degree of reliability combining the sensitivity of this heterostructure to the direction of application of the field and the strong magnetoresistive response.

Acknowledgements
Work supported by CICYT MAT 2008 06517.

Relaxation Characteristics of Low-molecular-weight Systems in Porous Host Matrix: Computer Simulation Study

S. Żurek[1], M. Kośmider[1], Z. Dendzik[2], K. Górny[2]

[1] *Institute of Physics, University of Zielona Góra*
Szafrana 4A, 65-516 Zielona Góra, Poland

[2] *Institute of Physics, University of Silesia*
Uniwersytecka 4, 40-007 Katowice, Poland

The effect of nano-scale confinement to the properties of molecules entrapped in porous materials is an interesting field of investigation in various research fields: biology, geology and material science, just to name a few [1–4].

One of the important questions there is: how the attracting interaction between the host (porous matrix) and the guest system (the molecule) counterbalances the confinement effect imposed by the geometrical constraints. The two effects influence the dynamics of the whole system and thus – manifest themselves in a dipolar relaxation process.

An analysis of the characteristics of such a relaxation process in the systems of molecules embedded in a porous host matrix is performed by a fully atomistic molecular dynamics simulation.

References

[1] U. Raviv and J. Klein 2001, *Nature* **413** 51
[2] K. Morishige and K. Kawano 1999, *J. Chem. Phys.* **110** 4867
[3] S. Mitra, R. Mukhopadhyay, I.Tsukushi and S. Ikeda 2001, *J. Phys.: Condens. Matter* **13** 8455
[4] P. Pissis, D. Daoukaki-Diamanti, L. Apekis and C. Christodoulides 1994, *J. Phys.: Condens. Matter* **6** L325

POSTERS

Hybrid Organic–Inorganic Nanosystems Based on Polypnenylacetylene and Fullerene Integrated with Porous Silicon Matrix

O. I. Aksimentyeva[1], L. S. Monastyrskyy[1], B. R. Tsizh[2], V. P. Savchyn[1], L. I. Yaryc'ka[3]

[1] *Ivan Franko Lviv National University*
6/8 Kyryla-Mefodia Str., L'viv, 79005, Ukraine

[2] *Kazimierz Wielki University in Bydgoszcz*
30 Chodkiewicza Str., Bydgoszcz, 85-064, Poland

[2] *L'viv State University of Safety in Vital Activity*
35 Kleparivska Str., L'viv, Ukraine

Heterostructures created on porous silicon (PS) and surface organic layers of which the conjugated conducting polymers, including in particular the polyaniline, have been intensively studied, are of great interest for the development of solar cells, light emitting diodes, sensors, lasers and memory devices [1, 2]. The effect of an integrated organic component on the molecular spectra and luminescence characteristics of the PS - polyphenylacetylene (PPA) and PS – fullerene C_{60} nanostructures was investigated in the present work.

The PPA and C_{60} layers on a porous silicon surface were obtained by dip-coating of a polymer (or fullerene) from a solution in an organic solvent. The structure of the obtained hybrid layers was studied by FT-IR spectroscopy and atom force microscopy (AFM). The emissive properties of hybrid layers were examined by photoluminescence excited by an LGI-21 pulse nitrogen laser ($\lambda = 337.1$ nm), and cathode luminescence (CL) at $T = 78$ K under excitation by a pulse electron flow with energy $E_p = 9$ keV, pulse frequency $f = 50$ Hz and $\tau_p = 3$ μs. The current density in the electron beam $j = 150$ A/m^2. The temperature of CL measurements was 80 K. The PS surface had a shape of vertical nanorods created due to the etching of separate places of a single silicon surface. Following a statistical analysis of the AFM-images it was defined that the pore depth achieved 150–180 nm with a total thickness of the porous layer of about 5 μm. The dip-coated fullerene and PPA layers obtained on the surface of PS repeated in general the surface relief forming a continuous polymer layer (Figure 1).

It was found that the existence of an organic component on a PS surface caused significant changes in the luminescence properties of nanostructures. In particular, the intensity of CL for the PS–PPA and PS-C_{60} hybrid layers significantly increased compared with the CL for PS without a polymer. The peak emission magnitude at $E = 2.22$ eV increased by a factor of 1.5 to 2.7 (for PS-PPA and PS-C_{60} heterostructures), while in the case of PS-C_{60} an additional intensive emission peak appeared at $E = 3.2$–3.4 V. According to the FT-IR spectroscopy the surface of PS obtained by

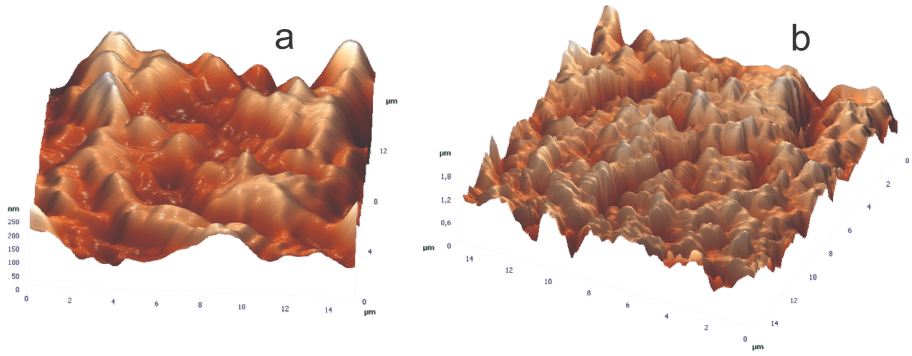

Figure 1: AFM image of surface topology for PS-C_{60} (a) and PS-PANI (b) hybrid structures obtained by dip-coation (a) and electropolymerization (b)

electrochemical treatment of single silicon in an HF alcohol solution contains the different functional groups with the absorption at 2900–3620 cm^{-1} (–OH), 1100 cm^{-1}, 1240 cm^{-1} (Si–O–Si), 1111 cm^{-1} (C–O), 1072 cm^{-1} (CH–OH), 620 cm^{-1} (Si–H_2) and others.

In the presence of an organic component (polymer or fullerene) an interaction of the organic component with porous silicon surfaces took place. The evidence of such an interaction were the shifts of the Si–O–Si absorption from 1100 and 1240 cm^{-1} to 1050 and 1250 cm^{-1}, also as the appearance of new bands with the maximums at 1188 (C–C), 1280 (Ar–OH) and 1770 (C=O) cm^{-1} which may be assigned to the formation of weak covalent bonds between the polymer or fullerene and the surface of a semiconductor. Having compared a relative increase in the CL emission heterostructures it can be assumed that the non-irradiative surface recombination rate decreases at the PS surface coating with a polymer due to the passivity of the film.

Apparently, this caused an increase in the radiative component of recombination as well as an increase in the CL intensity. However, further experimental and theoretical studies turn out to be necessary in order to elucidate the mechanisms of the occurrence of CL in heterostructures.

References

[1] Jayachandran, M., Paramasivam, M., Murali, K.R., Trivedi, D.C. 2001 *Mater. Phys. Mech.* 4 43

[2] Aksimentyeva O. I., Monastyrskyy L. S., Savchyn B. M., Stakhira P. Y, Vertsimakha Ya. I., Tsizh B. R. 2007 *Molec. Cryst. & Liq. Cryst.* 467 73

Structure and Magnetic Properties of Metal Organic Magnet Based on Iron Complex with 2-hydroxy-1-nitrozonaphthalene

O. I. Aksimentyeva[1], V. P. Dyakonov[2,3], S. Piechota[3], A. Shapovalov[2], H. Szymczak[3], B. R. Tsizh[4]

[1] *Ivan Franko Lviv National University*
6/8 Kyryla-Mefodia, L'viv, 79005, Ukraine

[2] *Donetsk Physical & Technical Institute NASU*
72 R. Luxemburg, Donetsk, 83114, Ukraine

[3] *Institute of Physics, Polish Academy of Sciences*
Al. Lotników 32/46, Warsaw, 02-668, Poland

[4] *Kazimierz Wielki University in Bydgoszcz*
30, Chodkiewicza, Bydgoszcz, 85-064, Poland

Investigations of magnetic properties of new metal-organic materials should favor the understanding of the magnetism nature in organic magnets. In the present report the structure, the temperature dependence of an EPR spectrum and the magnetic behavior of a metal-organic complex of iron with 2-hydroxy-1-nitrozonaphathalene $Na[Fe(C_{10}H_6ONO)_3]$ was investigated over the temperature range of 4.2–300 K.

An anionic complex of iron with 2-hydroxy-1-nitrozonaphathalene in the form of sodium salt was synthesized and characterized as described in [1]. According to IR, UV-spectroscopy, thermogravimetry and an elemental analysis the molecular formula of the complex salt $Na[Fe(C_{10}H_6ONO)_3]$ was confirmed. In this complex the ferric ion is surrounded by three nitrozonaphthole ligands and connected with nitrogen and oxygen atoms of each ligand to form pentagonal helat cycle. According to the X-ray powder diffraction data this complex salt has a low symmetry, its structure is monoclinic with the following lattice parameters: $a = 1.116$ nm; $b = 0.876$ nm; $c = 0.620$ nm; $\beta = 92.4°$.

An unusual temperature dependence in the EPR spectrum was manifested in this substance, being similar to polyaniline and polyparaphenylene doped by Fe^{3+} [2]. The EPR spectrum is a superposition of two lines with contrasting behavior with the changing temperature. When the temperature is lowered, the intensity of the first line increases and the intensity of the second line decreases, hence one line has the maximum intensity at low (helium) temperatures, the other – at room temperatures. The first line is a low-temperature (LT) EPR spectrum, the second line – a high temperature (HT) spectrum. A change in the temperature leads to a redistribution of the absorption intensities between the LT and HT spectra. This behavior of the EPR spectrum evidences the unusual dynamics of the molecules surrounding the magnetic

ion. The presence of this dynamics may cause substantial influence on the various properties of the metal organic substance.

The preliminary results of investigations of the DC magnetization and AC susceptibility show that this compound exhibits features which are characteristic of a spin-glass system.

References

[1] Aksimentyeva E. (O.) I., Dyakonov V. P., Shapovalov V. A., Piechota S. 2000 *Zurnal Obschei Khimii* **70** (10), 823

[2] Vasyukov V. N., Shapovalov V. A., Dyakonov V. P., Dmitruk A. F., Aksimentyeva E. I., Szymczak H., Piechota S. 2002 *Intern. J. Quantum Chem.* **88**, 525

FIB Nanopatterning for SiGe Nanostructures Self-assembly on Si Substrate

G. Amiard[1], I. Berbezier[1a], M. Aouassa[1], L. Favre[1], A. Ronda[1], C. Marcus[2], I. Alonso[2]

[1] *IM2NP, CNRS – Université d'Aix Marseille, Campus St Jérôme Case 142, 13397 Marseille CEDEX 20, France*

[a] *isabelle.berbezier@im2np.fr*

[2] *ICMAB-CSIC Campus de la UAB, 08193 Barcelona, Spain*

In the last decade, a significant progress has been made towards the development of new processes for integrating nanostructured materials into novel micro- and opto-electronic devices. The nanostructures of interest include arrays of clusters, nanoparticles, quantum dots and wires. For most of the potential applications the nanostructures must be ordered and highly homogeneous in size in order to exploit the quantum effects for device applications.

In the first part of the presentation, a review of the recent advances in self-assembly mechanisms and processes will be given [1]. The paper will particularly address the mechanisms of formation of highly ordered arrays of Ge quantum dots during the growth on nano-patterned Si(001) substrates [2,3].

The second part of the paper will be devoted to a new fabrication process of Ge nanocrystals (NC) embedded in an SiO_2 amorphous matrix. The two step fabrication process is based on Ge QD self-assembly on Si(001) substrate nanopatterned by Focused Ion Beam (FIB). During the first step, FIB direct writing is used to create an array of ultra-small holes in thin thermal SiO_2 layer on an Si(001) substrate. New results obtained with an Orsay Physics FIB apparatus implemented with an in situ mass filter and allowing high resolution nanopatterning with a gold ion beam will be presented.

References

[1] I. Berbezier, A. Ronda, *Surf. Sci. Rep.*, in press
[2] A. Pascale, I. Berbezier, A. Ronda, P. Kelires, *Phys. Rev. B* 075311 (2008)
[3] I. Berbezier, A. Ronda, *Phys. Rev. B* 195407 (2007)

Effect of Substitutions of Zn for Mn on Size and Magnetic Properties of Mn–Zn Ferrite Nanoparticles

A. Amirabadizadeh[1a], H. Farsi[2], H. Arabi[1], M. Dehghani[1]

[1] *Department of Physics, Faculty of Science, University of Birjand Birjand, Iran*

[2] *Department of Chemistry, Faculty of Science, University of Birjand Birjand, Iran*

[a] *ahmadamirabadi@yahoo.com*

In this study Mn-Zn ferrite nanoparticles ($Mn_{1-x}Zn_x$ Fe_2O_4, $x = 0, 0.3, 0.5$) were produced by the chemical co-precipitation method. It is the easiest and the most useful method to produce ferrite nanoparticles in the solution phase. Fe_2O_3 was dissolved in HCl to obtain Fe^{3+} ions in aqueous solutions. $MnCl_2$ $4H_2O$, and $ZnSO_4$ $7H_2O$ were used to obtain Zn^{2+}, Mn^{2+} ions in aqueous solutions. The solutions containing these ions were mixed in an appropriate molar proportion in distilled water. To prepare Mn-Zn ferrite nanoparticles the NaOH solution was added to the previous mixture at the temperature of 80°C. The structure and size of the Mn-Zn ferrite nanoparticles was characterized using X-ray diffraction (XRD) and Transmission Electron Microscopy (TEM). It was found that the size of Mn-Zn ferrite nanoparticles decreased with an increase in the Zn concentration. The magnetic properties of Mn-Zn ferrite nanoparticles were investigated with a vibrational sample magnetometer (VSM) and it was observed that $Mn_{0.7}Zn_{0.3}Fe_2O_3$ ferrite nanoparticles had the maximum saturation magnetization and that the initial susceptibility decreased with an increase in the Zn concentration.

Wavefunction-Engineering of Intersubband THz-Laser Nanoheterointerfaces

E. A. Anagnostakis

Nanotechnology Focus; Alimos, Greece
22 Kalamakiou Ave., GR 174 55 Alimos, Greece
emmanagn@otenet.gr

A novel THz-luminescence LASER nanoheterointerface operational principle of the intersubband longer-wavelength limit mid-infrared functionality type is designed on the basis of optically pumped dual resonant tunnelling of conductivity electrons within an appropriately energetically determined scheme of five subbands hosted by two communicating asymmetric approximately rectangular quantum wells (QWs).

The upper LASER action level employed is the second excited subband of the nanostructure back wider QW which is provided with electrons via resonant tunnelling from the first excited subband of the nanostructure front QW populated through remotely ignited optical pumping out of the local fundamental subband.

On the other hand, the first excited back QW subband functions as the lower LASER action level, directly delivering the received electrons to the local fundamental subband – via fast vertical longitudinal optical phonon scattering, wherefrom they are recycled back to the nanostructure front QW fundamental subband by virtue of a second – reverse sense – resonant tunnelling – mediated normal charge transport mechanism.

The ensuing calculations incorporate the determination of effective dipole lengths associated with intersubband transitions collaborating or antagonising with one another through the optoelectronic structure, the intersubband transition lifetime engineering thus emerging as a conformal mapping of the original heterosturcture wavefunction-engineering attempted. Furthermore, the determined intersubband transition (ISBT) effective dipole lengths demonstrate the oscillator strengths supporting different ISBT events, whereas the predicted LASER action population inversion leads to the device stimulated optical gain.

Formation and Ordering of Si and Ge Dots by Dewetting

M. Aouassa[1,2], I. Berbezier[1a], L. Favre[1], G. Amiard[1], A. Ronda[1], H. Maaref[2], A. Miranda[3], P. D. Vedova[3], F. Traversi[3], R. Sordan[3]

[1] *IM2NP, CNRS – Université d'Aix Marseille, Campus St Jérôme Case 142, 13397 Marseille CEDEX 20*

[a] *isabelle.berbezier@im2np.fr*

[2] *LPSCE, Faculté des Sciences de Monastir Avenue de l'environnement 5019, Monastir, Tunisie*

[3] *LNESS, Polo di Como, Politecnico di Milano, Italy*

Recently, a morphological instability of silicon-on-insulator (SOI) films has been observed during the processing of devices using ultra-thin SOI films. This instability leads to the transformation of 2D silicon films into an array of isolated 3D islands. This transformation results from the surface energy driven phenomenon which drives the system to reduce the interfacial area due to the high Si–SiO_2 interfacial energy. The morphological evolution of the 2D silicon layer has been described in the literature by a multisteps process including:

1) the heterogeneous nucleation of voids;
2) the thickening of the dewetted edges;
3) the extension of the dewetted areas by propagation of wavy "fingers" voids;
4) the agglomeration of crystalline silicon under the form of droplets by breaking up the dewetted front.

In this study, we first describe the dynamics of Silicon dewetting as a function of time, temperature and silicon thickness. SOI samples with Si top layers 8 and 16 nm thick were annealed at temperatures between 700°C and 850°C in an ultra-high vacuum chamber and observed by AFM, SEM and cross-section TEM. In all the samples, the dewetted area, the shape of the voids and the distribution, size and morphology of 3D islands were investigated. The results show that the voids nucleation occurs randomly on the surface (and not preferentially at the edges of the samples). The voids have circular shapes with dendritic edges and a denuded centre zone (absence of islands). There is no material piling up on the edges of the voids although this agglomeration was expected to be at the origin of the islands formation in the models (due to capillary instability). This absence of edges thickening is attributed to the immediate smoothing produced by a large surface diffusion. We also show that the rate of extension of the dewetted areas is controlled by diffusion even though holes nucleation continues to occur. A systematic analysis of the droplets

morphology and orientation evidences a shape transformation during dewetting, where islands first elongate along the dewetted front and then rotate to adopt the equilibrium shape of silicon with (111), (113) and (100) facets. This shape transformation is not accompanied by crystallographic planes rotation and all the 3D islands keep their initial crystallographic orientation matching the substrate orientation.

In the second part of the study, we develop a two-step process based on a combination of pre-patterning and dewetting to fabricate self-assembled silicon (or germanium) islands. Ultra-thin SOI layers are pre-patterned by *e*-beam lithography to create arrays of holes and of lines oriented along the [100] and [110] crystallographic directions and penetrating up to the oxide layer. When the distance between the patterns matches the size of the islands, a perfect ordering of the Si islands is obtained. The best result is obtained when arrays of holes are formed along [100] with a 500 nm periodicity. In this situation, only one island is formed between four holes. When the patterns consist of an array of lines, during annealing the islands first elongate along the lines and then rotate towards the crystallographic directions. Moreover, the *e*-beam pre-patterning of the surface before dewetting dramatically increases the NCs size and shape homogeneity and allows for a perfect control of the NCs position. This two-step process has also been used for the formation of periodic arrays of ultra-small Si and Ge dots for photovoltaic applications.

Role of Processing in Structure–Function Relationship of Polymeric Bulk Heterojunction Solar Cells

D. Bagnis[1a,2], L. Valentini[1], A. Facchetti[2], T. J. Marks[2], J. M. Kenny[1]

[1] *Civil and Environmental Engineering Department, University of Perugia Strada Pentima Bassa 4, Terni, Italy*

[a] *diego.bagnis@unipg.it*

[2] *Department of Chemistry, Catalysis Center, Northwestern University 2145 Sheridan Road, Evanston IL, U.S.A.*

In the recent years the growing interest in exploitation of renewable energy has led the researchers to develop both new materials to achieve higher power conversion efficiencies and new deposition techniques to achieve the industrialization of these products.

Great interest has been shown in photovoltaic devices based on organic semiconductors such as π-conjugated molecules [1–3] due to their solution processability, their compatibility with plastic substrates and low temperature processes as, for example, roll-to-roll and ink-jet manufacturing technologies. The principle of bulk heterojunction solar cells [4–10] (BHJ) based on the spontaneous phase separation between donor and acceptor materials has become popular leading to the development of high-performance devices by using a dispersion of [6,6]-phenyl C_{61}-butyric acid methyl ester (PCBM) as the acceptor material within regioregular poly(3-hexylthiophene) [6].

A wide range of parameters such as the film structure at the nanoscale level and the interface phenomena must be carefully controlled to obtain high quality BHJ devices from solution casting. The most important aspects are the evaporation kinetic of the solvent, the deposition temperature and the environmental conditions. These factors determine the mobility of charge carriers in the active material and the degree of interpenetration of the phase-separated domains.

We report here a systematic study on the structure-function relationship of BHJ solar cells depending on several experimental parameters such as the solvent and the thermal annealing procedure adopted. We have also demonstrated that the interface between the donor (i.e. polymer) and acceptor (i.e. PCBM) phases depends on the deposition technique used; for example, we have found how the dip-coating technique results in ordered surface lamellar domains (Figure 1) which leads to a power conversion efficiency of 3.6%.

In conclusion, we have investigated the role of the solution casting techniques as methods for production of polymeric BHJ solar cells. A combination of this class of

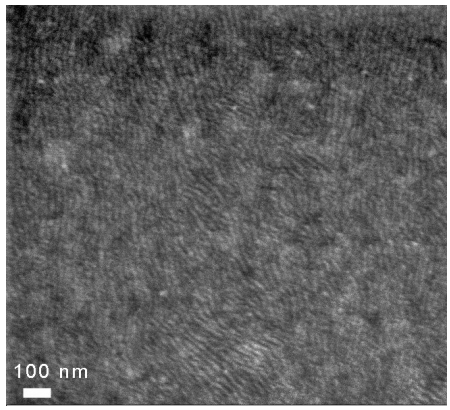

Figure 1: SEM image of a thin layer of a P3HT/PCBM blend deposited by the dip-coating technique

materials with the optimization of the processing methods should lead to the development of integrated technologies that could bring an opportunity of producing high efficiency photovoltaic devices on an industrial scale.

References

[1] Yu, G.; Gao, J.; Hummelen, J. C.; Wudl F.; J.Heeger, A. *Science* **1995**, *270*, 1789
[2] Brabec, C. J.; Sariciftci N. S.; Hummelen J. C. *Adv. Funct. Mater.* **2001**, *11*, 15
[3] Sariciftci, N. S.; Smilowitz, L.; Heeger A. J.; Wudl, F. *Science* **1992**, *258*, 1474
[4] Blom, P. W. M.; Mihailetchi, V. D.; Koster, L. J. A.; Markov, D. E. *Adv. Mater.* **2007**, *19*, 1551
[5] Gunes, S.; Neugebauer, H.; Sariciftci, N. S. *Chem. Rev.* **2007**, *107*, 1324
[6] Reyes-Reyes, M.; Kim, K.; Dewald, J.; Lopez-Sandoval, R.; Avadhanula, A.; Curran, S.; Caroll, D. L. *Org. Lett.* **2005**, *7*, 5749
[7] Brabec, C. J.; Cravino, A.; Meissner, D.; Sariciftci, N. S.; Fromherz, T.; Rispens, M. T.; Sanchez, L.; Hummelen, J. C. *Adv. Funct. Mater.* **2001**, *11*, 374
[8] Li, G.; Yao, Y.; Yang, H.; Shrotriya, V.; Yang, G.; Yang, Y. *Adv. Funct. Mater.* **2007**, *17*, 1636
[9] Berson, S.; De Bettignies, R.; Bailly, S.; Guillerez, S. *Adv. Funct. Mater.* **2007**, *17*, 1377
[10] Li, G.; Shrotriya, V.; Huang, J.; Yao, Y.; Moriarity, T.; Emery, K.; Yang, Y. *Nat. Mater.* **2005**, *4*, 864

Nonlinear Impedance as an Indication of Ionpolaron Interraction in Cu_2O–Al_2O_3–SiO_2 Glass

R. J. Barczyński

Faculty of Applied Physics and Mathematics, Gdansk University of Technology
Narutowicza 11/12, 80-233 Gdansk, Poland

jasiu@mif.pg.gda.pl

In terms of response, signal linearity impedance measurements may be classified as two sorts: linear and nonlinear methods. Usually it is only linear measurements that are performed and it is a small amplitude excitation that is employed to guarantee linearity. A large excitation may cause nonlinearities. It is a good assumption for conventional systems where there are no intrinsic nonlinearities and nonstationary processes. For more complicated situations nonlinear (and nonstationary) impedances may contain more complete information than the conventional impedance. Unfortunately, due to the lack of established methods of analysis and appropriate software such measurements are rather uncommon.

Some copper oxide glasses exhibit mixed electronic-ionic conductivity [1]. Electronic conduction occurs by small polaron hopping between Cu^+ and Cu^{2+} ions. On the other hand, the movement of Cu^+ ions is responsible for ionic conductivity. Such a situation implies nonlinearities: the movements of ions change the distribution of the hopping centers while the polaron hopping process influences the concentration of mobile Cu^+ ions. Both processes modify each other in a complicated way and the impedance should not be considered linear any more.

One member of the family of glasses containing copper oxide is the Cu_2O–Al_2O_3–SiO_2 glass. The aim of the present study was to find more clues on the possible interaction between electronic and ionic conductivity in the $12.5Cu_2O$–$12.5Al_2O_3$–$75SiO_2$ (in mol %) glass by means of nonlinear impedance spectroscopy. The obtained results show that a large nonlinearity in the impedance signal is observed at moderate electric fields of an order of 1 V/mm. The contents of the third harmonics reach about 10% and strongly depends on the temperature and frequency.

References

[1] R. J. Barczyński, L. Murawski *J. NonCryst. Solids* 307310 (2002) 1055

AC and DC Conductivity in $V_2O_5P_2O_5$ Glasses Containing Alkaline Ions

R. J. Barczyński[a], P. Król, L. Murawski

Faculty of Applied Physics and Mathematics, Gdansk University of Technology
Narutowicza 11/12, 80-233 Gdansk, Poland

[a] *jasiu@mif.pg.gda.pl*

Glasses containing a large amount of transition metal oxides exhibit electronic conductivity. Their electrical properties are determined by the presence of transition metal ions in two different valence states and the conductivity is described by a mechanism of small polaron hopping between such ions. When alkali ions are introduced, mixed electronicionic conductivity phenomena are observed in these glasses. Ionic conduction generally depends on the alkali concentration and carrier ions mobility. Assuming that the motions of alkali ions and polarons are independent one may expect that the electrical conductivity should increase with an increase in the alkali content. However, real transition metal oxide glasses containing alkali show very various types of electrical behavior ranging from strong anomalies in conductivity of several orders of magnitude at certain amounts of alkali ions to conductivity that is only very little dependent on the alkali content [1].

The aim of the present work is to investigate the AC and DC conductivity in $50V_2O_5$–$(50-x)P_2O_5$–xA_2O (A = Li, Na, K) systems as a function of temperature and composition. The measurements were carried out in the frequency range from 10^4 to 10^7 Hz. For all compositions, the DC conductivity measured at room temperature decreased with the increasing alkali ion content. The decrease in conductivity was larger for heavier alkali ions and reached more than four orders of magnitude in the case of glass containing 40 mol % of Na_2O. The AC conductivity exhibited universal dynamic response described as Jonscher's power law: $\sigma_{\mathrm{AC}} = A\omega_{s(T)}$.

For glasses containing less than 10 mol % of alkaline ions, the temperature dependence of the exponent $s(T)$ was typical as for electronic conducting glasses and decreased from a value near to unity at low temperatures (153 K) to 0.5 at 423 K. In the mixed electronicionic regime observed in glasses containing 20, 30 and 40 mol % Na_2O or K_2O only small variation (from 0.99 to 0.95) of $s(T)$ was observed. An almost linear dependence of the AC conductivity corresponded to a nearly frequency independent dielectric loss. This behavior is known as nearly constant loss (NCL) regime and was observed in some ionic conducting glasses at low temperatures and high frequencies [2]. We have found that in mixed electronic ionic conducting glasses the NCL behavior can be observed in a very wide range of temperature and frequency.

References

[1] L. Murawski, R. J. Barczyński *Solid State Ionics* 176 (2005) 2145
[2] B. Roling, C. Martiny, S. Murugavel *Phys. Rev. Letters* 87 (2001) 0859011

Influence of Iron Additives on Semiconduction Properties of Al-based Amorphous Metallic Alloys

L. Bednarska[1], M. Kovbuz[1], A. Budniok[2], J. Kubisztal[2], J. Panek[2], M. Popczyk[2]

[1] *Ivan Franko National University of L'viv*
Kyryla and Mefodiya 6, 79005, L'viv, Ukraine

[2] *Institute of Materials Science, University of Silesia*
12 Bankowa, Katowice, 40-007, Poland

New amorphous alloys on the basis of aluminium, $Al_{87}Gd_5Ni_8$ and $Al_{87}Gd_5Ni_4Fe_4$, were studied in this work. These alloys were synthesized at the Institute of Metal Physics of the National Academy of Sciences of Ukraine (Kiev) for current research purposes and for further practical applications, in particular. The aim of this work was to study the corrosive properties of AMA and to determine the relationship between the composition of AMA and the semiconducting properties of protective layers on the surface of alloys. In order to accomplish this aim a complex of physico-chemical methods, namely the potentiometry, voltammetry, electrochemical impedance spectroscopy and electronic microscopy were used.

The passivation of aluminium alloys is set by a dense oxide layer which forms on their surface and terminates further corrosion. The introduction of different doped additives to a composition of Al-based AMA upgrades the corrosion properties of these materials and changes the type of conduction (hole or electron) of the oxide coating which has perspective application significance. The redox processes of $Al_{87}Gd_5Ni_8$ and $Al_{87}Gd_5Ni_4Fe_4$ were studied by the cyclic voltammetry method in a 0.1 M NaCl aqueous solution. It was determined that the partial replacement of nickel (4 at. %) by iron led to a decrease in the corrosion current and to an increase in the polarization resistance which pointed to a higher corrosion resistance of $Al_{87}Gd_5Ni_4Fe_4$. The formation of oxide passivation layers on the AMA-electrodes was studied by the electrochemical impedance spectroscopy method in the 0.1 M NaCl aqueous solution. The choice of the impedance model for the formation of an oxide (AMA) | 0.1 M NaCl (aq.) and AMA | 0,1 M NaCl (aq.) phase boundary was carried out. It was determined that active diffusion reactions which could be described by the Warburg element proceeded on the porous oxide ($Al_{87}Gd_5Ni_4Fe_4$ AMA) | 0.1 M NaCl (aq.) boundary. The Mott-Schottky relationships were plotted and the semiconductor nature of the formed oxide coatings was determined on the basis of the impedance measurements. It was shown that the addition of iron to the alloys composition changed their conductivity from the *p*- to *n*-type. The determination of the semiconductor type which forms on the Al-based amorphous alloys surface, offers a scope for the programming adsorption of bioactive compounds that is an important medical-biological problem today.

Carbon Nanotube Cuckypaper: Low Toxicity and Decreased Proliferation of Human Cancer Cell Lines

S. Bellucci

INFN-Laboratori Nazionali di Frascati, Via E. Fermi 40, 00044 Frascati, Italy

Buckypaper, an innovative material with interesting prospects in pharmacology and prosthetics is studied in terms of its effects on cancer and primary cell lines *in vitro*. It is shown that it induces a decrease in the proliferation of human colorectal, breast and leukemic cancer cell lines, having, at the same time, no effect on the proliferation and viability of normal human arterial smooth muscle cells and human dermal fibroblasts. Taking into account the precautions needed when carbon nanotubes are injected into human body for drug delivery, as well as in medical diagnostics, or as the basic material for prosthetic applications, and given the structural resemblance of buckypaper to asbestos, whose toxicity has been linked to cancer, we assessed the buckypaper toxicity, both *in vitro* and *in vivo*. On laboratory rats, buckypaper induces a moderate inflammatory reaction but has no mutagenic effects. The animals, after buckypaper implantation, showed an inflammatory reaction followed in the next two weeks by the cicatrisation reaction with the organization and the fibrosis of the scar. The results obtained show low buckypaper toxicity both *in vitro* and *in vivo*.

References

[1] S. Bellucci (2009). Nanoparticles and Nanodevices in Biological Applications. The INFN Lectures – Vol I. BERLIN HEIDELBERG: Springer Verlag, vol. 4, p. 1–198, ISBN: 978-3-540-70943-5.

[2] M. Chiaretti, G. Mazzanti, S. Bosco, S. Bellucci, A. Cucina, F. Le Foche, G. A. Carru, S. Mastrangelo, A. Di Sotto, R. Masciangelo, A. M. Chiaretti, C. Balasubramanian, G. De Bellis, F. Micciulla, N. Porta, G. Deriu and A. Tiberia, Carbon nanotubes toxicology and effects on metabolism and immunological modification in vitro and in vivo, J. Phys.: Condens. Matter **20** (2008) 474203 (10pp)

[3] M. De Nicola, S. Bellucci, E. Traversa, G. De Bellis, F. Micciulla and L. Ghibelli, Carbon nanotubes on Jurkat cells: effects on cell viability and plasma membrane potential, J. Phys.: Condens. Matter **20** (2008) 474204 (9pp)

[4] A. Di Sotto, M. Chiaretti, A. Carru, S. Bellucci, G. Mazzanti, Multi-Walled Carbon Nanotubes: lack of mutagenic activity in the bacterial reverse mutation assay, Toxicology Letters, (2009) bf 184 pp. 192–197, ISSN: 0378-4274, doi:10.1016/j.toxlet.2008.11.007

[5] B. M. Rotoli, O. Bussolati, M. G. Bianchi, A. Barilli, C. Balasubramanian, S. Bellucci and E. Bergamaschi, Non-functionalized multi-walled carbon nanotubes alter the paracellular permeability of human airway epithelial cells, Toxicology Letters Volume **178**, Issue 2, 5 May 2008, Pages 95–102

[6] S. Bellucci, M. Chiaretti, A. Cucina, G. A. Carru, A. I. Chiaretti, Multiwalled carbon nanotube buckypaper: toxicology and biological effects *in vitro* and *in vivo*, Nanomedicine (2009) **4** (5), 531–540

Dispersed CeO_2 in Cobalt: a Way to Improve the Coating Properties

L. Benea[1a], P. Ponthiaux[2], F. S. Sorcaru[1], F. Wenger[2]

[1] *Dunărea de Jos University of Galati*
Competences Center: Interfaces-Tribocorrosion-Electrochemical Systems
(CC-ITES), 47 Domneasca Street, RO-800008 Galati, Romania

[a] *Lidia.Benea@ugal.ro*

[2] *Ecole Centrale Paris, Laboratoire Génie des Procédées Matériaux (LGPM)*
F-92290 Châtenay-Malabry, France

Composite materials are material systems that consist of a discrete constituent (reinforcement) distributed in a continuous phase (matrix) and that derive their distinguishing characteristics from the properties and behaviour of their constituents.

Most composite coatings contain micron-sized particles. The major challenges with the codeposition of second phase particles are the nano-sized particles co-deposition, the achievement of a high level of codeposition and avoiding an agglomeration of particles suspended in electrolytes. The homogeneously poor distribution of second phase particles in a metallic matrix can be detrimental to the all properties.

This work shows the most recent results regarding the influence of CeO_2 bioceramic dispersed in a cobalt matrix during an electroplating process on the surface morphology and corrosion behaviour of the nanocomposite coatings obtained.

Recent studies indicate that cerium oxide particles can function as biological antioxidants due to their ability to switch between different oxidation states. Cobalt and

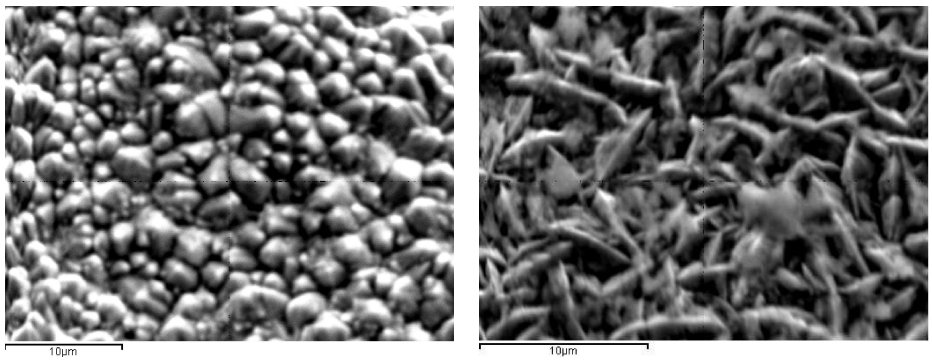

Figure 1: Left panel: SEM surface morphology of pure cobalt electroplating obtained at 23 mA/cm^2 (×2000); right panel: SEM surface morphology of CeO_2/Co nanocomposite coatings obtained at 23 mA/cm^2 (×2000)

its alloys are already used as metallic implants in medicine, dental implants, surgical implants, bone regeneration / replacement. The aim of our work is to obtain CeO_2/Co nanocomposite coatings by an electroplating process with improved properties compared to pure cobalt.

Pure cobalt and CeO_2/Co nanocomposite coatings were electrochemically deposited from a sulphate – chloride electrolytic bath. The mean diameter of CeO_2 dispersed particles was 20 nm. The CeO_2 nanoparticles could be electrocodeposited with cobalt to obtain composite coatings. The surface morphology of nanocomposite coatings had a fine and uniform surface structure.

CeO_2 had influence on the structure and properties of the Co matrix which was due to the amount of CeO_2 embedded in the matrix.

CeO_2 particles in the Co matrix decrease by increasing the current densities used for electrocodeposition.

Influence of Nano SiC Co-deposition with Nickel to Biofilm Formation on Nanocomposite Coatings

L. Benea[1a], A. Ciubotariu[1], B. Tribollet[2], W. Sand[3]

[1] *Dunarea de Jos University of Galati*
Competences Center Interfaces – Tribocorrosion and Electrochemical Systems (CCITES)
47 Domneasca St., 800008 Galati, Romania

[a] *Lidia.Benea@ugal.ro*

[2] *Laboratoire Interfaces et Systemes Electrochimiques*
Université Pierre et Marie Curie, Paris France

[3] *University of Duisburg-Essen, Biofilm Centre, Aquatic Biotechnology*
Duisburg, Germany

Bacteria adhesion is a very complicated process affected by many factors: bacterial/material properties and environment. The effect of these parameters on bacterial adhesion can be evaluated by surface modification. A rigorous study of the effects of surface chemistry/topography on bacterial adhesion and protein adsorption requires a model system that would allow precise control of the type and configuration of functional groups at the substrate surface under dynamic conditions. Regarding the environment it was observed that bacterial concentration versus the time of exposure increased with the increasing bacterial concentration and time, up to a saturation level, specific for each type of the surface-bacterial strain. The concentration of electrolytes, CO_2, pH and ionic strength depend on bacteria and material surface characteristics. Accordingly the presence of antibiotics decreases depending on bacterial susceptibility and antibiotics concentrations. All these factors may influence bacterial adhesion by either changing the physical interactions in phase one of adhesion, or by changing the surface characteristics of bacteria or materials. The bacterial characteristics influence also the biofilm formation and growth. Hydrophobic bacteria prefer hydrophobic material surfaces. The Materials Characteristics and Chemistry of surfaces are the most important factors in bacterial adhesion and biofilm growth. Cells initially attach by physico-chemical interactions or extracellular matrix protein secretion to form a cell monolayer in which cells express pili and have a twitching motility and/or the ability to undergo chemotaxis. Cells proliferate in the monolayer and other microbes [attach to this monolayer. to form an active biofilm, the development and distortion of which is influenced by environmental factors such as hydrodynamic and mechanical stress. Cells in a mature biofilm are motile and undergo chemotaxis which leads to the spreading of biomass and an increased horizontal gene transfer rate. As cells die, active bioconversion and/or biodegradation lead to a solute transfer to or from the bulk liquid which results in eventual biofilm detachment. The work was focussed on performing surface modification studies by co-deposition of dispersed particles with metals in order to observe the influence of the materials structure (nano-

and micro-structured coatings prepared) on the bacteria cells (Sulphate Reducing Bacteria) attachment. Sessile bacteria on coupons were stained with 4, 6-diamidino-2-phenylindol (DAPI) and visualized by EFM as well as AFM. In order to complete the investigations of the properties of SiC-nickel nanostructured coatings the samples were also tested for biological marine corrosion in the presence of SRB. The solution test was natural marine seawater enriched with very aggressive sulphate reducing bacteria. These types of bacteria are well known as very corrosive for metals in natural seawater. Epifluorescence microscopy (EFM) imaging of a DAPI – stained biofilm sample of SRB on the surface of nickel and SiC/Ni nano composite coatings obtained are presented in Figures 1–2.

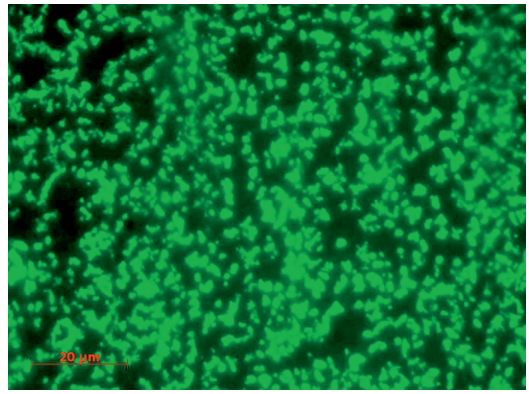

Figure 1: Fluorescence microscope image of SRB on pure nickel surface obtained at a current density of 4 A/dm^2, 60 min

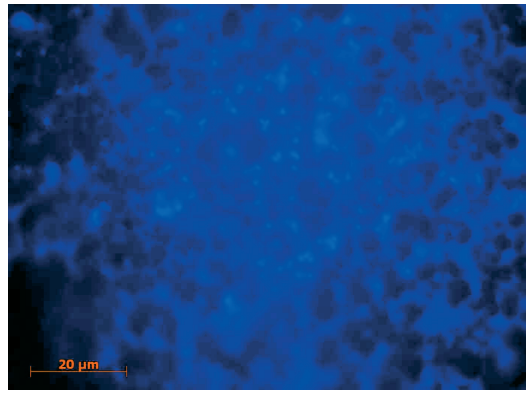

Figure 2: Fluorescence microscope image of SRB on SiC/Ni nano composite coatings surface obtained at a current density of 4 A/dm^2, 60 min

Nanofiber Organic Solar Cells: Device Performance and Active Layer Morphology

S. Bertho[1], W. D. Oosterbaan[1], V. Vrindts[2], J. D'Haen[1], T. J. Cleij[1], L. Lutsen[2], J. Manca[1,2], D. Vanderzande[1,2]

[1] *Hasselt University, Institute for Materials Research*
Wetenschapspark 1, B-3590 Diepenbeek, Belgium

[2] *IMEC vzw, IMOMEC*
B-3590, Diepenbeek, Belgium

Within the field of organic bulk heterojunction solar cells, the morphology of the active layer has a key role in obtaining high power conversion efficiencies. It has been shown that P3HT (poly(3-hexylthiophene)) nanofibers, obtained in highly concentrated solutions, are able to give improved morphologies directly upon deposition [1,2]. In this work, P3AT's (poly(3-alkylthiophene)) with side chains ranging from 4 carbon atoms to 9 carbon atoms (further denoted as P34T to P39T) were used as the electron donor material in polymer:PCBM bulk heterojunction solar cells. For each material, nanofibers in highly concentrated solutions were prepared according to [3].

For P36T, it has been shown that the photovoltaic performance of the fiber solar cells depends on the fiber content (= fiber part of the P3AT fraction) in the casting solution [1,2]. Here, the fiber content was varied by changing the temperature of the casting solution [4]. By increasing the solution temperature, the fiber content decreased. In this way, an optimization of the photovoltaic performance was obtained easily for each P3AT. When comparing the P3AT's with the different side chains, the widely used P36T still gave the best photovoltaic performance (about 3.2%) after this optimization (Figure 1).

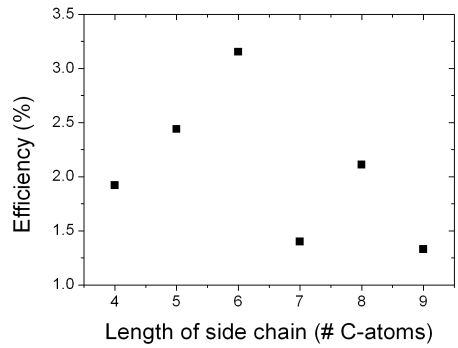

Figure 1: Efficiencies obtained from nanofiber-P3AT:PCBM solar cells, the side chain length of the nanofiber-P3AT ranged from 4 to 9 carbon atoms

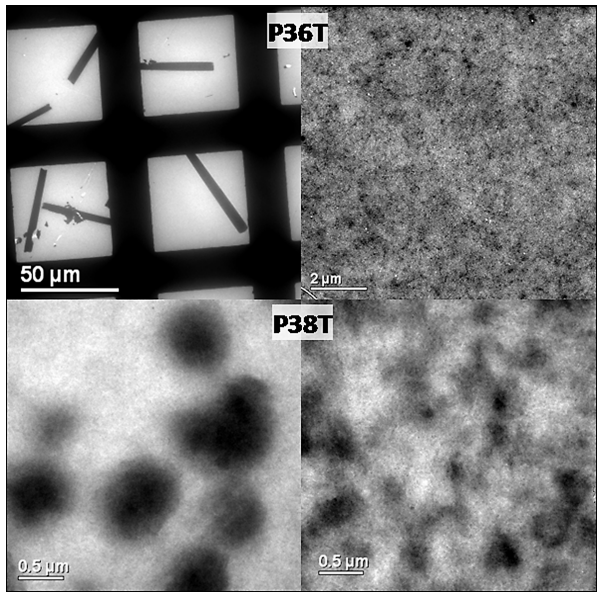

Figure 2: BFTEM images of the polymer:PCBM active layers (the dark regions represent PCBM)

Transmission Electron Microscopy (TEM) was used to study the active layer morphology. Not only the fiber content, but also the dissolution of PCBM appeared to be a crucial part in the fabrication of good devices. Bright Field TEM images show that at low solution temperatures (Figure 2, left), PCBM grouped into large (> 50 μm) needles for P36T and into circular chunks (~ 0.5 μm) for P38T.

The optimal performance of the photovoltaic devices was found at slightly higher temperatures where, on the one hand, PCBM was dissolved properly to give a more homogeneous mixture with the polymers (Figure 2, right), and on the other hand, the fiber content in the solution was high enough to provide beneficial charge transfer properties.

Acknowledgements
The research was carried out in the framework of the SBO-project 030220 'PolySpec' and the FWO-project R-1226 'Nanofibre'. Sabine Bertho is research assistant of the Fund for Scientific Research, Flanders (Belgium) (FWO).

References

[1] Berson S, De Bettignies R, Bailly S, Guillerez S 2007 *Adv. Funct. Mater.* **17** 1377
[2] Moulé A J, Meerholz K 2008 *Adv. Funct. Mater.* **20** 240
[3] Oosterbaan W D, Vrindts V, Berson S, Guillerez S, Douhéret O, Ruttens B, D'Haen J, Adriaensens P, Manca J, Lutsen L, Vanderzande D *J. Mater. Chem.* in press. DOI: 10.1039/b900670b
[4] Bertho S, Oosterbaan W D, Vrindts V, D'Haen J, Cleij T J, Lutsen L, Manca J, Vanderzande D *Org. Electron.* in press. DOI: 10.1016/j.orgel.2009.06.018

Tensile Strength of Carbon Nanotubes

M. Białoskórski[1], J. Rybicki[1,2]

[1] *TASK Computer Centre*
Narutowicza 11/12, 80-233 Gdansk, Poland

[2] *Department of Solid State Physics*
Faculty of Technical Physics and Applied Mathematics
Gdansk University of Technology
Narutowicza 11/12, 80-233 Gdansk, Poland

Extensive classical Molecular Dynamics simulations of tensile strength of single-walled carbon nanotubes have been performed using the AIREBO force field. About 230 nanotubes of radii from 2.1 Å ($(0,5)$ nanotube) to 13.3 Å ($(20,20)$ nanotube) have been simulated systematically and the dependence of their tensile strength and stiffness moduli on the nanotube's radius has been determined. It turns out that (n,n) nanotubes are more mechanically resistant that $(n,0)$ nanotubes.

Annealing Effect on EPR Spectra of Ti–Si–C–N System Samples

N. Guskos[1,2], E. A. Anagnostakis[3], G. Żołnierkiewicz[2], J. Typek[2], A. Biedunkiewicz[4], A. Guskos[2]

[1] *Solid State Section, Department of Physics, University of Athens Panepistimiopolis, 15 784 Zografos, Athens, Greece*

[2] *Institute of Physics, West Pomeranian University of Technology Al. Piastów 48, 70-311 Szczecin, Poland*

[3] *Department of Computer and Communication Engineering, University of Thessaly, Deligiorgi Building, 382 21 Volos, Greece*

[4] *Institute of Materials Science and Engineering, West Pomeranian University of Technology Al. Piastów 19, 70-310 Szczecin, Poland*

Two nanocrystalline samples (TiC_x + SiC)/C were prepared by the non-hydrolytic sol-gel method. The second sample was subjected to additional annealing at high temperature. The XRD measurements showed the presence of aggregates of cubic SiC+TiC nanoparticles (10 to 30 nm in size). In both samples a very narrow electron paramagnetic resonance (EPR) line arising from magnetic localized centers was centered at g_{eff} of about 2 (the differences in the resonance fields of both samples were 0.6 Gs). At $T = 130$ K linewidths $\Delta H_{\text{pp}} = 1.41(2)$ Gs and $\Delta H_{\text{pp}} = 2.92(2)$ Gs were registered for a sample without and with thermal annealing, respectively. For the non-annealed sample the resonance line could be fitted by the Lorentzian line in a higher temperature region and by a Dysonian line below 70 K which suggested an essential change in the electrical conductivity. For the annealed sample the resonance line-shape was Dysonian in the whole investigated temperature range. Thus, the thermal annealing process could improve significantly the transport properties. An analysis of the temperature dependence of the EPR parameters (g-factor, linewidth, integrated intensity) showed that the thermal annealing processes essentially influenced the re-orientation processes of the localized magnetic centers.